ELSEVIER

PII: S0011-2275(97)00139-2

Cryogenics **38** (1998) 169–176

Printed in Great Britain
0011-2275/98/$19.00

Numerical simulation and experimental verification of the oscillating flow in pulse tube refrigerator

Y.L. Ju*, C. Wang and Y. Zhou

Cryogenic Laboratory, Chinese Academy of Sciences P. O. Box 2711, Beijing, 100080, China

Received 31 March 1997; revised 17 July 1997

An improved numerical modeling for simulating the oscillating fluid flow and detail dynamic performance of the orifice and double-inlet pulse tube refrigerator has been developed in this paper. The governing equations that include the pressure gradient, inertia, viscous and convection terms are based on the conversion of mass, energy and momentum for oscillating flow in refrigerator. The full implicit time-dependent and upwind second-order finite difference scheme are used to discrete the governing equations. Simulation results and predicated performance are compared with the experimental data. Good agreement has been found between the two. Detail time-dependent axial wall temperature distribution, transient gas temperature, mass flow rate and dynamic pressure variations in the pulse tube refrigerator have been obtained in this paper. The simulation model is useful for understanding the physical process occurring in the pulse tube refrigerator, and also for predicting the effect of the orifice and double-inlet valve on the refrigeration power and efficiency of pulse tube refrigerator.

Keywords: numerical simulation; experimental verification; pulse tube refrigerator

Nomenclature

A	Cross-sectional area of pulse tube
A_o	Cross-sectional area of orifice
c_p	Specific heat at constant pressure
d_0	Diameter of orifice
d_1	Diameter of double-inlet
D_h	Hydraulic diameter of pulse tube
e	Specific internal energy
E	Total internal energy
f	Friction factor, frequency
h	Specific enthalpy
H	Total enthalpy
k	Ratio of specific heat
$\dot{m}$	Mass flow rate
P	Pressure
q	Heat flux
R	Gas constant
Re	Reynolds number
t	Time
T	Temperature
u	Velocity
V	Volume
W	Compressor work
α	Heat transfer coefficient
θ	Crank angle
λ	Thermal conductivity
ρ	Density
τ	Period time
μ	Correction factor of the nozzle
σ	Visious stress
Φ	Dependent variable vector

Subscripts

c	Cold end
d	double-inlet
h	Hot end
o	Orifice
p	Pulse tube
r	Regenerator
s	Solid matrix of regenerator
v	Double-inlet
w	Wall
0	Initial
1	Cold end of the pulse tube
2	Hot end of the pulse tube

*To whom correspondence should be addressed

Introduction

The need for cryogenic cooling of space-base electronics, infrared detectors and the associated electronics has brought about a strong requirement for the developments of high reliability and efficiency in refrigerators. Pulse tube refrigerators first discovered by Gifford and Longsworth[1], which contains no moving parts at its cold end, so it has considerable system advantages over most other types of refrigerators in reliability, lifetime, vibration, and cost. The developments and innovations[2–6] achieved in recent years enable pulse tube refrigerator to have a comparable refrigeration capability with Stirling or G-M machines. Detail review of the works done on the pulse tube refrigerator can be found in references[7–9].

The working process of the pulse tube refrigerator is very complex due to the unsteady, oscillating compressible gas flow, the porous media in regenerator and the addition of the orifice valve and double-inlet valve, etc. Many previous analysis of the pulse tube refrigerator are based on the method of enthalpy flow and phase analysis reported by Storch and Radebaugh[10]. However, the quantitative accuracy of the analytical results was not satisfactory. An understanding of the mechanisms associated with pulse tube refrigerator requires a full solution of the Navier-Stokes equations. However, the complexity of these equations make an analytical solution for pulse tube refrigerator essentially impossible. Therefore, numerical methods have been usually employed to simulate the oscillating process. The numerical modeling presented by Wu and Zhu[11], Zhu and Chen[12] neglected the pressure drop in the regenerator, so it was impossible to obtain satisfactorily quantitative results. Wang et al. published a set of numerical papers[13–15] which included the gas flow friction and heat transfer in the heat exchanger and regenerator. Their results showed that the gas flow friction cannot be neglected since it caused phase and amplitude differences in pressure in the different parts of the refrigerator. However, the momentum equation for the regenerator in their model does not have the natural characteristics of conservation form and neglects the momentum equation of gas flow in the pulse tube.

In the present study, an improved numerical modeling for simulating the detail dynamic performance and characteristics of the oscillating flow in the pulse tube refrigerator has been developed. Numerical simulation is performed to study the effects of the orifice valve and double-inlet valve on the performance of the pulse tube refrigerators. The predicated simulation results are compared with the experimental data obtained by a pulse tube refrigerator developed by Cryogenic Laboratory. Good agreement was found between the two. Detailed time-dependent axial wall temperature distribution, transient gas temperature, mass flow rate and dynamic pressure variations in the pulse tube refrigerator have been obtained in this paper.

Physical model and governing equations

A valveless pulse tube refrigerator is shown in *Figure 1a*, which includes compressor 1, aftercooler 2, regenerator 3, cold end heat exchanger 4, pulse tube 5, hot end heat exchanger 6, orifice 7, reservoir 8, and double-inlet valve 9. The working medium is helium. In the present study, if the double-inlet valve 9 closed, the model is a conventional orifice pulse tube. Pulse tube and regenerator length, is much longer than the typical hydraulic diameter in the cross-section of pulse tube. The variation in the thermal properties and momentum in the radial direction seems to have little effect on the behavior of the pulse tube refrigerator. Therefore, the one-dimensional model has been adopted for numerical simulation to reduce the CPU time and avoid any difficulty involved with the two- or three-dimensional models. For the sake of simplicity, it is assumed that the valve opening remains circular as the flow area of the valve is varied. Neglecting any geometric complexity in regenerator, simulation of the pulse tube refrigerator carried out for the simplified one-dimensional physical model is shown in *Figure 1b*. The basic assumptions are as follows:

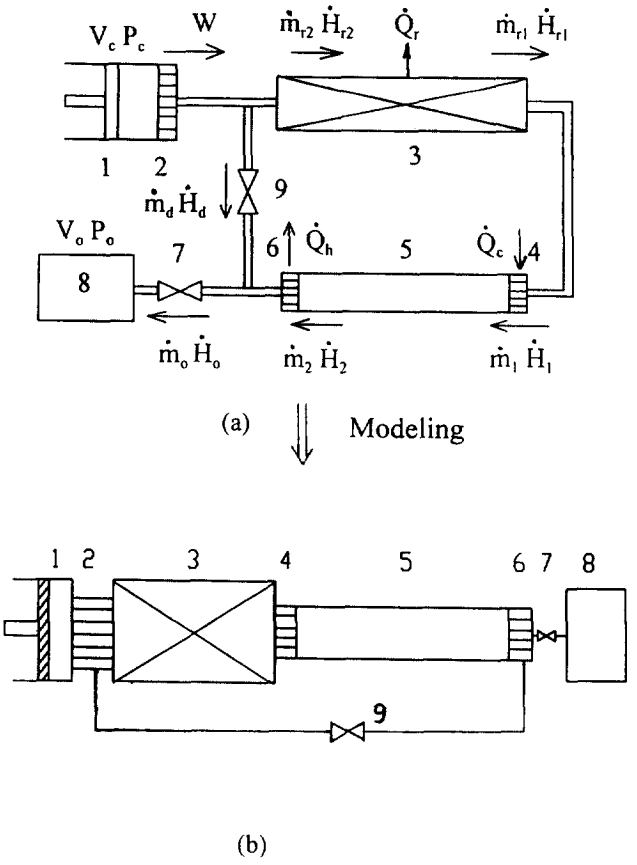

Figure 1 Schematic of the physical model for the pulse tube refrigerator 1. compressor; 2. aftercooler; 3. regenerator; 4. cold end heat exchanger; 5. pulse tube; 6. hot end heat exchanger; 7. orifice; 8. reservoir; 9. double-inlet valve

1. one-dimensional laminar compressible flow
2. the gas and porous medium in regenerator are in local thermal equilibrium
3. the porous medium is incompressible, uniform porosity
4. boundary and variable permeability effects are negligible

The governing equations that include the pressure gradient, inertia, viscous and convection terms are based on the conservative forms of mass, energy and momentum for oscillating flow, which is usually used in the numerical simulation of compressible fluid flow is the following:

$$\frac{\partial E}{\partial t} + \frac{\partial F}{\partial x} + G = 0 \tag{1}$$

where:

$$E = \begin{bmatrix} \rho \\ \dot{m} \\ E \end{bmatrix} \quad F = \begin{bmatrix} \rho u \\ \dot{m}u + P \\ u(E+P) \end{bmatrix} = \begin{bmatrix} \rho u \\ \dot{m}u + P \\ \rho u h \end{bmatrix}$$

$$G = \begin{bmatrix} 0 \\ \sigma \\ S \end{bmatrix} \quad \sigma = f\frac{\rho}{2D_h}|u|u \quad S = \frac{\partial q}{\partial x} \quad q = \alpha(T - T_w)$$

here u is the velocity, $\dot{m}$ is the mass flow rate, $u = \dot{m}/\rho$, E is the total internal energy, $E = \rho(e + uu/2)$, and $H = \rho h = E + P$ is the total enthalpy, h is the specific enthalpy

Equation of state:

$$h = f(P,T) \tag{2}$$

Assuming simple sinusoidal oscillations for the compressor, so the compressor volume change with crank angle is

$$V = V_d + 1/2V_S(1 + \cos 2\pi ft) \tag{3}$$

where V_d is the dead volume and V_S is the swept volume

It should be noted that the mass flow rate is defined as positive if the gas flows from the compressor to the reservoir and as negative for the opposite flow. The mass flow rate through the orifice an double-inlet valves are determined using a formula for the convergent nozzle with a correction factor

$$\dot{m}_o = \mu A_o \sqrt{2\frac{k}{k+1}\frac{P}{V}\left[\left(\frac{P_b}{P}\right)^{2/k} - \left(\frac{P_b}{P}\right)^{(k+1)/k}\right]}$$

$$(P > P_b) \tag{4}$$

$$\dot{m}_o = \mu A_o \sqrt{2\frac{k}{k+1}\frac{P_b}{V_b}\left[\left(\frac{P}{P_b}\right)^{2/k} - \left(\frac{P_b}{P}\right)^{(k+1)/k}\right]}$$

$$(P > P_b)$$

μ is correction factor, which is determined by the experimental data.

The initial conditions are given as follows

$$t = 0: T = T_S = T_0,\ P = P_0,\ \dot{V} = \dot{V}_d + \dot{V}_S \tag{5}$$

It is reasonable to assume constant wall temperature of the hot and cold end heat exchangers, and the working process in the reservoir to be a constant temperature. The boundary conditions are given as follows

$$T_{w2} = T_{w6} = T_8 = T_h,\ T_{w4} = T_c \tag{6}$$

Friction factor and heat teansfer coefficients

Since we could not find the friction fact and heat transfer coefficient for the oscillating gas flow, and the transition from laminar to turbulent flow is not obvious in the pulse tube refrigerators, we adopted the steady friction factor and heat transfer coefficient from reference[16]. The friction factor is

$$f = \Gamma(f_1, f_2) \tag{7}$$

where the function Γ is defined as the largest among the variables, that is $\Gamma(x,y) = \max 0(x,y)$

$$f_1 = 1.6 + 180/Re \tag{8}$$

$$f_2 = 0.257Re^{-0.157} \tag{9}$$

The heat transfer coefficient is

$$\alpha = \Gamma(\alpha_1, \alpha_2) \tag{10}$$

$$\alpha_1 = \frac{0.023\lambda Re^{0.8}Pr^{0.4}}{D_h} \tag{11}$$

$$\alpha_2 = \frac{1.47\lambda Re^{0.536}Pr^{0.333}}{D_h} \tag{12}$$

Numerical methods and procedure

The above set of differential equations are non-linear and unsteady. Considering the non-continuity of interface temperature at various parts in the pulse tube refrigerator, the complex heat and fluid flow boundary, the conjugate thermal conduction and convection between the gas flow and the solid matrix in regenerator, and the large temperature gradient in the regenerator and pulse tube, some effects have been made to improve both the calculation accuracy and speed. The governing equations are discretized using a control-volume approach by the inter node method as described by Patankar[17]. We adopted the staggered grid approach to eliminate the mistaken pressure profiles, as shown in *Figure 2*. This approach uses control volumes for the velocities that are staggered with respect to those for temperature and pressure.

A solution is obtained from an initial guess through an iterative scheme using a line-by-line TDMA (tri-diagonal matrix algorithm) method. The governing equations are solved with SLUR and block correction technique, the upwind second-order scheme for the dependent variables (as discussed later), harmonic mean formulation for the interface diffusivities. The conjugate thermal conduction and convection between the gas and the solid matrix in the regenerator are handled numerically by solving the same full set of momentum and energy equations throughout the entire pulse tube refrigerator, but with a large value of viscosity specified for solid matrix, details of the technique can be found in Patankar[17]. Since thermal physical proper-

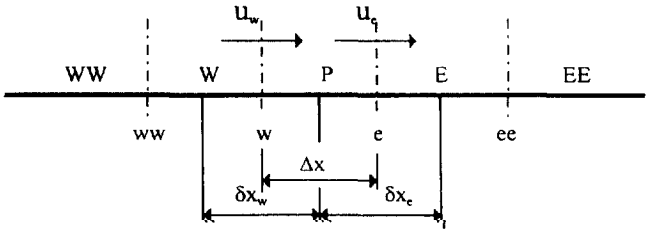

Figure 2 The schematic of the staggered grid

ties (thermal conductivity and viscosity) vary with temperature and pressure, the compute table has been established and these thermal properties are calculated by interpolation within the table during the numerical calculation.

In our model, independent variables are the density, mass flow rate, pressure, and temperature.

A general numerical scheme for Equation (1) in *Figure 2* can be written as

$$E_P^{n+1} = E_P^n + \lambda\theta(F_e^{n+1} - F_w^{n+1}) - \lambda(1-\theta)(F_e^n - F_w^n) + G_P^n \tag{13}$$

where, $\lambda = \Delta t/\Delta x$, the superscripts n and n + 1 represent time levels, and θ is a measure of implicitness of the scheme. We can obtain explicit, fully implicit, and Crank-Nicolson schemes for θ = 0,1 and 1/2 respectivity. F_P are the numerical fluxes at the control-volume interfaces. A general expression for the upwind second-order scheme at the interface can be written as:

$$F_e^{(1)} = \frac{1}{2}(F_P + F_E) - \frac{1}{2}\Gamma\left[\frac{1}{2}(F_E - F_P), -\frac{1}{2}(F_E - F_P)\right] \tag{14}$$

$$F_e^{(2)} = F_e^{(1)} + \frac{1}{2}[(F_P - F_w) + (F_E - F_{ee})] \tag{15}$$

where the function Γ is defined as the largest among the variables, that is $\Gamma(x,y) = \max 0(x,y)$

To increase the calculation accuracy and convergence, the source term can be written as:

$$S = S_C + S_P\phi_P \tag{16}$$

Equation (13) can be differentiated and rewritten by using the TDMA (tri-diagonal matrix algorithm) method, we can obtain the standard formula for the TDMA method as follows

$$a_P\phi_P = a_W\phi_W + a_E\phi_E + b \tag{17}$$

$$a_P = a_W + a_E - S_P \tag{18}$$

$$b = S_C + a_P\phi_P^0 \tag{19}$$

where $\Phi = \dot{m},T,P$. Φ^0 is the value obtained by the previous converged solutions for last iteration, which is at the under-relaxation term:

$$a_P\phi_P = a_W\phi_W + a_E\phi_E + b + (1-\alpha)a_P\phi_P^0 \tag{20}$$

Computational accuracy and convergence rate are affected by the orifice and double-inlet valves. In order to improve the simulation accuracy, the mass flow rate through the orifice and double-inlet valve calculated by the mass conservation equation is corrected by Equation (4).

The iteration results should be satisfied by periodic stable conditions for all the time-dependent parameters and the energy balance condition for the matrix of the regenerator during a cycle. The convergence criteria is:

$$\frac{|\phi(\theta) - \phi(\theta + 2\pi)|}{|\phi(\theta)|} < \epsilon \tag{21}$$

After a grid refinement study, all calculations presented here were carried out using a 200 non-uniform grid size, the calculated results with finer grid do not reveal noticeable changes. The grid is finer for the pulse tube and regenerator volume near the heater exchanger in order to identify effectively the shape gradient of temperature profile. The solution was obtained through the entire pulse tube refrigerator, from compressor to reservoir. With the oscillating compressible gas flow condition and the conjugate thermal conduction and convection between the gas flow and the solid matrix in regenerator, the solution took a long time to obtain a convergent solution, requiring 200 ~ 300 CPU min on HP 5/90C mainframe. Use of previous converged solution at different conditions reduce the run times somewhat.

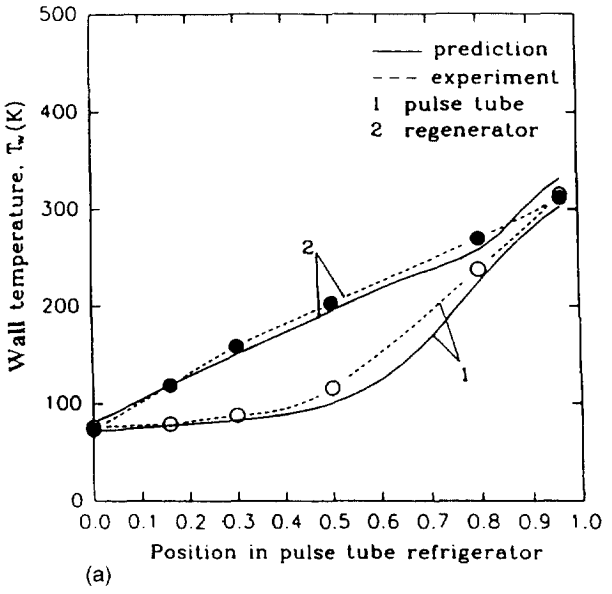

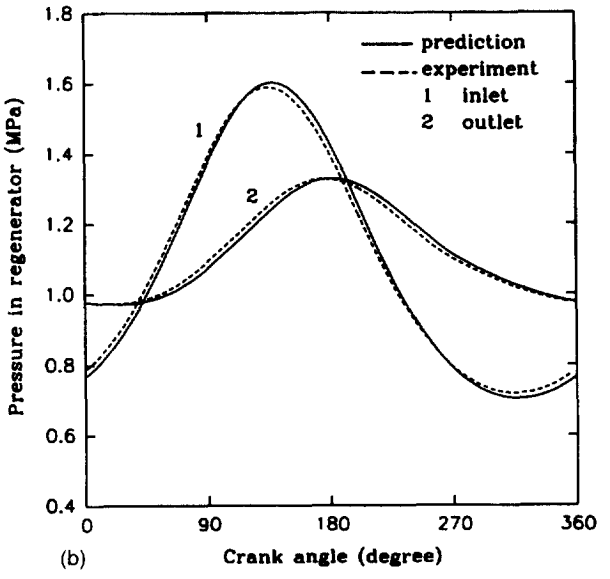

Figure 3 Comparison of the predicted simulation results with experiment (d_0 = 0.5 mm, d_1 = 0.5 mm). (a) time-average wall temperature distributions; (b) dynamic pressure in pulse tube

Table 1 Dimensions of each part of the regenerator and pulse tube

Component	Regenerator	Pulse tube
First part	∅17 mm × 80 mm	∅12 mm × 85 mm
Second part	∅14 mm × 58 mm	∅10 mm × 60 mm
Third part	∅10 mm × 55 mm	∅7.5 mm × 50 mm

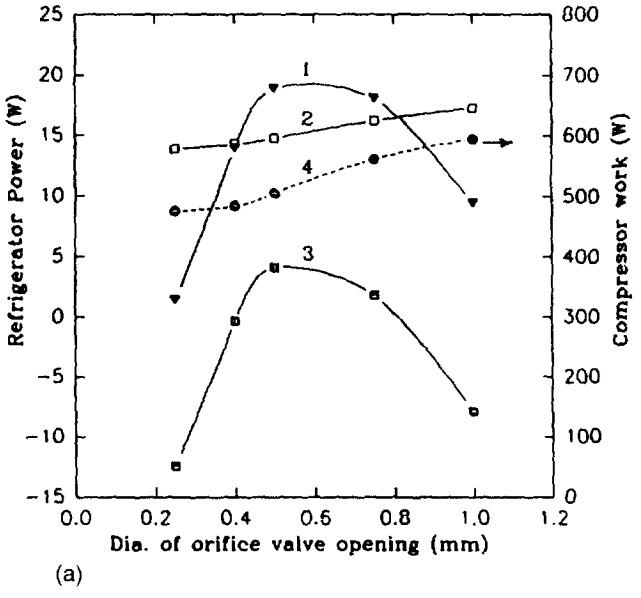

(a)

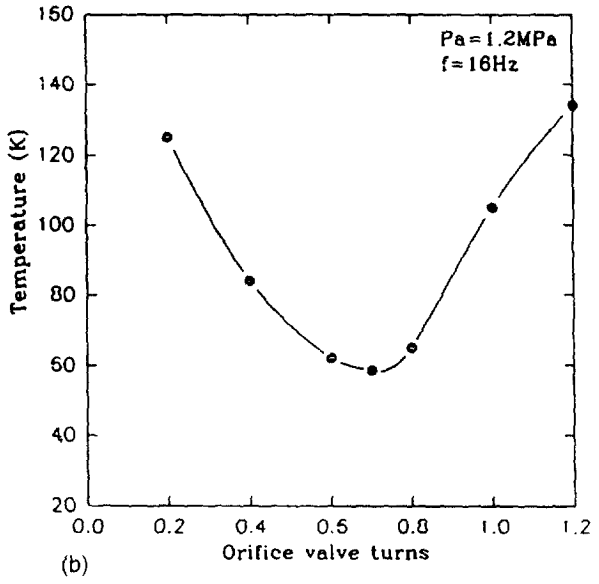

(b)

Figure 4 (a) Prediction of refrigeration power with orifice opening values (b) Experimental data of no load cold end temperature with orifice opening values

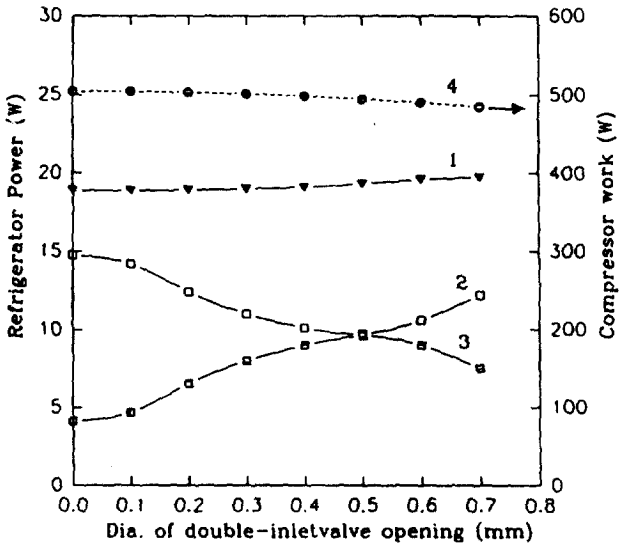

(a)

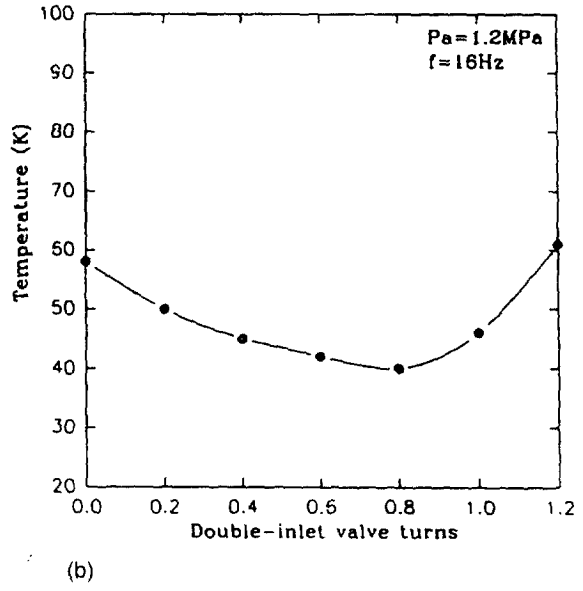

(b)

Figure 5 (a) Prediction of refrigeration power with double-inlet opening value (b) Experimental data of no load cold end temperature with double-inlet opening values (d_0 = 0.5 mm)

Comparison with experiment

Verification of our numerical modeling was carried out by comparing the simulation results to the experimental data. The test machine was a pulse tube refrigerator constructed at Cryogenic Laboratory. The configuration of the experimental apparatus was the same as *Figure 1a*. This apparatus utilized a valveless compressor which produced a sinusoidal pressure wave. The swept volume of the compressor was 55.6 cm^3 the compressor rotating speed was 960 rpm, so the frequency was 16 Hz; A reservoir volume of 300 cm^3 was connected to the hot end of pulse tube through an orifice valve, a double inlet valve was used between the hot end of the pulse tube and the regenerator, the orifice valve and the double inlet valve were all adjustable needle valves. The pulse tube and the regenerator were made of stainless steel with thickness of 0.25 mm. Considering that the gas

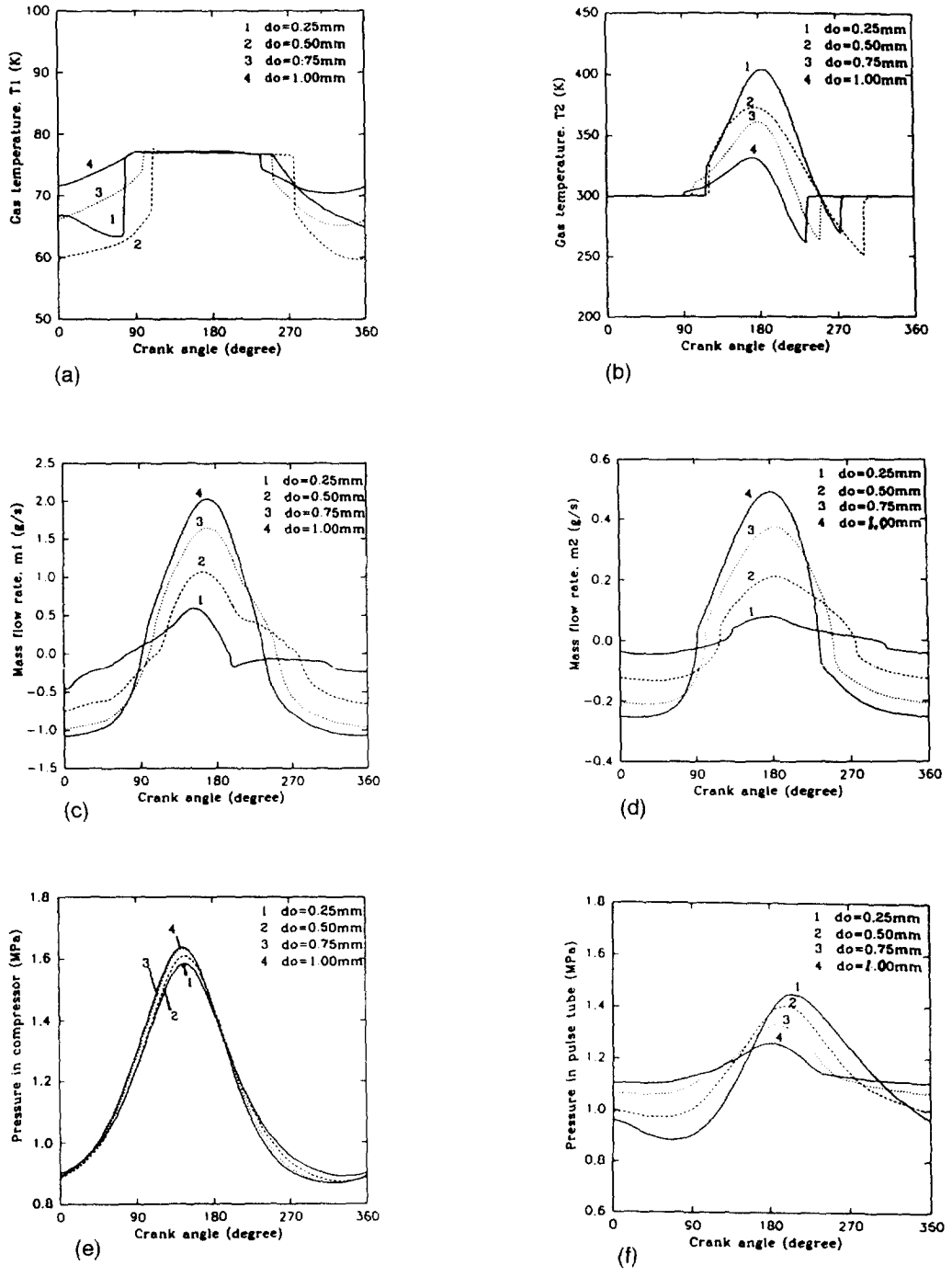

Figure 6 Variations of the temperature, mass flow rate, and dynamic pressure with the orifice opening values. (a) temperature at cold end pulse tube; (b) temperature at hot end pulse tube; (c) mass flow rate at cold end pulse tube; (d) mass flow rate at hot end pulse tube (e) dynamic pressure in the compressor; (f) dynamic pressure in the pulse tube

density and viscosity vary greatly with the temperature in the refrigerator, the pulse tube and the regenerator were separated into three parts, respectively. The dimensions of each parts of pulse tube refrigerator are given in *Table 1*. The regenerators were packed with phosphor bronze screens and stainless steel screens. Two small piezoresistive pressure transducers to measure the dynamic gas pressure wave were placed at the hot ends of the pulse tube and regenerator. A Rh-Fe thermometer was used to measure the temperature of the cold end of the pulse tube refrigerator, the measuring current was supply by DC power supply made by Lake Shore Cooperation. Ten cooper-constantan thermocouples were used to measure the wall temperature of the pulse tube and the regenerator. A heater resistance was provided at the cold end for cooling capacity measurement at a particular temperature.

A typical calculation has been made for pulse tube refrigerator whose main size is the same as the experimental rig. The main parameters are as follows: the operating wall temperature of the cold and hot end heat exchangers are 77 K and 300 K, respectively. The operating mean pressure is 1.2 MPa, the frequency f = 16 Hz. The predicted time-average wall temperature distributions of the pulse tube and regenerator, and dynamic pressure in the pulse tube refrigerator are compared to the experimental data as shown in *Figure 3a* and *b*, respectively. The results

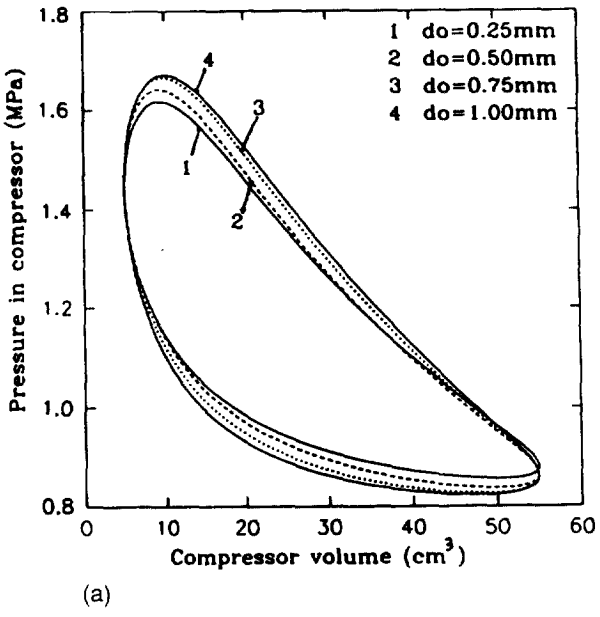

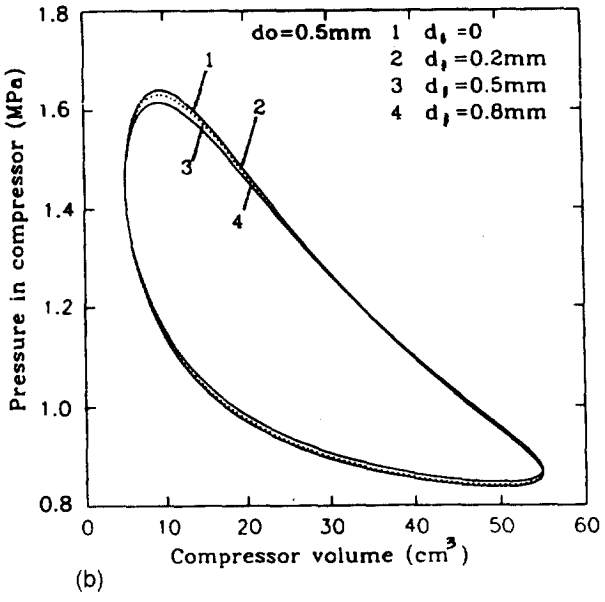

Figure 7 Variation of the compressor P-V work with the opening of the valve (a) the orifice opening values; (b) the double-inlet opening values

from the numerical simulation show reasonable agreement to the experimental data. *Figures 4* and *5a* are plots of the predicted refrigeration power of the orifice pulse tube refrigerator and double-inlet pulse tube refrigerator, respectively. Curve 1 in the figures is the refrigeration power obtained by neglecting pressure drop (neglecting the pressure gradient in Equation (1)) in pulse tube refrigerator; curve 3 is the refrigeration power calculated by our numerical modeling; curve 2 is the losses obtained by curve 3 minus curve 1; and curve 4 is the compressor work. The compressor work is defined as:

$$W = \frac{1}{\tau} \oint PdV \qquad (22)$$

Experimental data of no load cold end temperature are shown in *Figure 4b* and *Figure 5b*, in which the no load cold end temperature is plotted as a function of the valve opening. Optimum opening values of the orifice valve and double-inlet valve close to the middle range can clearly be seen in the figures. At the optimum valve opening, it is clear to see the low temperature in the experiment corresponds to the maximum refrigeration power in numerical simulation. Good agreement has been found between the predicted results and experimental data.

Computational result and discussion

Figures 6 and *7* show the dynamic characteristics of the pulse tube refrigerator as a function of run time, including instantaneous temperatures and mass flow rate at cold and hot end, dynamic pressure in compressor, regenerator and pulse tube, and compressor PV work.

Figure 6a–f show the effects of the orifice opening values on the dynamic parameters in the pulse tube refrigerator. *Figure 6a* and *b* show the instantaneous temperature variations at the two ends of the pulse tube for different orifice opening values. The cold end temperature of the pulse tube refrigerator achieve low temperature at the orifice opening value of d_0 = 0.5 mm. The larger the orifice opening value, the lower the temperature of hot end temperature. *Figure 6c* and *d* give the mass flow rate at the two ends of the pulse tube for different orifice opening values. The orifice opening has large effect on the mass flow rate, a larger opening valve tends to result in a high mass flow rate. While the double-inlet opening has little effect on the mass flow rate in our numerical simulation. The dynamic pressure in the compressor and in the pulse tube for different opening values of the orifice valve are shown in *Figure 6e* and *Figure 6f*. The pressure wave in the compressor remains almost the same for different orifice opening values, while the pressure wave in pulse tube decreased with the increased of the orifice opening. These results are in good agreement with experiments[18] and other numerical modeling[13].

The compressor PV work diagrams are plotted in *Figure 7a* and *b*. It should be noted that the compressor PV work increases with the opening of the orifice valve and decreases slightly with the opening of the double-inlet valve. This agree with the results given in References [13,14].

From the figures above, it can be seen that the effect of the orifice and the reservoir is not only a phase shift but an amplitude shift. According to the numerical simulations and experiment, there exists an optimum opening value of the orifice valve for producing the maximum refrigeration power.

Conclusions

An improved numerical modeling for simulating the oscillating flow and detail dynamic performance of a pulse tube refrigerator has been developed. Good agreement has been found between the numerical simulation and experimental data. Detailed time-dependent axial wall temperature distribution, transient gas temperature variations, mean mass flow rate and dynamic pressure distribution of the oscillation flow in the pulse tube refrigerator have been obtained in this paper. The simulation model is useful for under-

standing the dynamic parameters and physical process occurring in the pulse tube refrigerator, and also for predicting the effect of the orifice and double-inlet valve on the refrigeration power and efficiency of pulse tube refrigerator.

Acknowledgements

The research work is supported by the National Natural Science Foundation of China.

References

1. Gifford, W.E. and Longsworth, R.C., Pulse tube refrigeration. *Trans. ASME, No. 63-WA-290*, 1963, pp. 264.
2. Mikulin, E.I., Tarasov, A.A. and Shrebyonock, M.P., Low-temperature expansion pulse tube. *Adv. Cryo. Eng.*, 1984, **29**, 629.
3. Zhu, S., Wu, P. and Chen, Z., Double inlet pulse tube refrigerator-An important improvement. *Cryogenics*, 1990, **30**, 514.
4. Zhou, Y. and Han, Y.J., Pulse tube refrigerator research. Proc. 7th. *Int. Cry. Conf. USA*, 1992, **7**, 147.
5. Ishizaki, Y. and Ishizaki, E., Experimental study and medellization of pulse tube refrigerator below 80 K down to 23 K.. *Proc. 7th Int. Refrigerator Conf. USA*,, 1993, **7**, 140.
6. Matsubara, Y. and Gao, J.L., Novel configuration of three-stage pulse tube refrigerator for temperatures below 4 K. *Cryogenics*, 1994, **34**, 259.
7. Radebaugh, R., A review of pulse tube refrigeration. *Adv. Cry. Eng.*, 1990, **35**, 1191.
8. Radebaugh, R., Recent developments in refrigerators.. *19th Int. Conf. Refrig.*, 1995, **19**, 973.
9. Chan, C.K., et al., Advanced pulse tube head development. *Proc. 9th Int. Refrig. Conf. USA*, 1996, **1**, 147.
10. Storch, P.J. and Radebaugh, R., Development and experimental test of an analysis model of the orifice pulse tube refrigerator. *Adv. Cry. Eng.*, 1988, **1**, 851.
11. Wu, P.Y. and Zhu, S.W., Mechanism and numerical analysis of orifice pulse tube refrigerator with a valveless compressor. *Proc. Int. Conf. Cryo. and Refrig.*, 1989, **3**, 85.
12. Zhu, S., Wu, P. and Chen, Z., Isothermal model of pulse tube refrigerator. *Cryogenics*, 1994, **34**, 591.
13. Wang, C., Wu, P.Y. and Chen, Z.Q., Numerical modeling of an orifice pulse tube refrigerator. *Cryogenics*, 1992, **32**, 785.
14. Wang, C., Wu, P.Y. and Chen, Z.Q., Numerical analysis of a double-inlet pulse tube refrigerator. *Cryogenics*, 1993, **33**, 526.
15. Wang, C., Cai, J.H., Zhou, Y. and Wang, S.Q., Numerical analysis and experimental verification of multi-bypass pulse tube refrigerator. *Adv. Cry. Eng.*, 1996, **41B**, 1389.
16. Kays, W.M. and London, A.L., Compact Heat Exchangers, 2nd McGraw-Hill, New York, USA, 1964.
17. Patankar, S.V., Numerical Heat Transfer and Fluid Flow, Hemisphere/2McGraw-Hill, New York, USA, 1980.
18. Cai, J.H., Zhou, Y., Wang, J.J. and Zhu, W.X., Experimental analysis of the double-inlet principle in pulse tube refrigerator. *Cryogenics*, 1993, **33**, 522.